A Physiologically Based Pharmacokinetic Analysis of Capecitabine, a Triple Prodrug of 5-FU, in Humans: The Mechanism for Tumor-Selective Accumulation of 5-FU

Yuko Tsukamoto,[1] Yukio Kato,[3] Masako Ura,[2] Ikuo Horii,[1] Hideo Ishitsuka,[2] Hiroyuki Kusuhara,[3] and Yuichi Sugiyama[3,4]

Received February 3, 2001; accepted April 20, 2001

Purpose. To identify the factors governing the dose-limiting toxicity in the gastrointestine (GI) and the antitumor activity after oral administration of capecitabine, a triple prodrug of 5-FU, in humans.
Method. The enzyme kinetic parameters for each of the four enzymes involved in the activation of capecitabine to 5-FU and its elimination were measured experimentally *in vitro* to construct a physiologically based pharmacokinetic model. Sensitivity analysis for each parameter was performed to identify the parameters affecting tissue 5-FU concentrations.
Results. The sensitivity analysis demonstrated that (i) the dihydropyrimidine dehydrogenase (DPD) activity in the liver largely determines the 5-FU AUC in the systemic circulation, (ii) the exposure of tumor tissue to 5-FU depends mainly on the activity of both thymidine phosphorylase (dThdPase) and DPD in the tumor tissues, as well as the blood flow rate in tumor tissues with saturation of DPD activity resulting in 5-FU accumulation, and (iii) the metabolic enzyme activity in the GI and the DPD activity in liver are the major determinants influencing exposure to 5-FU in the GI. The therapeutic index of capecitabine was found to be at least 17 times greater than that of other 5-FU-related anticancer agents, including doxifluridine, the prodrug of 5-FU, and 5-FU over their respective clinical dose ranges.
Conclusions. It was revealed that the most important factors that determine the selective production of 5-FU in tumor tissue after capecitabine administration are tumor-specific activation by dThdPase, the nonlinear elimination of 5-FU by DPD in tumor tissue, and the blood flow rate in tumors.

KEY WORDS: physiologically based pharmacokinetic model; capecitabine; 5-FU; tumor selective accumulation; blood flow rate.

INTRODUCTION

Capecitabine (N^4-pentyloxycarbonyl-5′-deoxy-5-fluorocytidine, Xeloda®), an orally administered triple prodrug of 5-FU, is sequentially metabolized to 5-FU by carboxylesterase, cytidine deaminase (cyd deaminase), and thymidine phosphorylase (dThdPase), which show relatively specific organ expression (Fig. 1) (1). By design, the biotransformation of capecitabine to 5′-deoxy-5-fluorocytidine (5′-DFCR) is intended to occur preferentially in the liver, compared with the gastrointestine (GI), to minimize the accumulation of 5-FU in the GI. Conversion of 5′-deoxy-5-fluorouridine (5′-DFUR) to 5-FU occurs via dThdPase, which is more highly expressed in many types of human tumors than in healthy tissues (Fig. 1). The 5-FU that is converted (anabolized) to active metabolites, fluorouridine triphosphate (FUTP), and fluorodeoxyuridine triphosphate (FdUTP), produced from capecitabine in this way, exhibits an anti-tumor effect. In humans, 60–90% of 5-FU is catabolized by dihydropyrimidine dehydrogenase (DPD) to dihydroxyfluorouracil (FUH_2) (2), whereas 10–20% is excreted in urine in the unchanged form (3).

Based on the above concept, capecitabine is expected to limit the exposure of the GI to 5-FU and allow preferential activation to 5-FU in malignant tumors. In a clinical study, the mean tumor to plasma 5-FU concentration ratio and that of tumor to adjacent healthy tissue were 21 and 3, respectively, after oral administration of capecitabine, demonstrating that capecitabine is preferentially activated in colorectal tumor tissue compared with healthy tissue (4). However, the therapeutic index (the ratio of 5-FU exposure of the target organ to the organ where capecitabine's adverse events have been observed) may not be influenced only by such tissue-specific expression of the metabolic enzymes, but also by other factors, including the tissue distribution of DPD, organ weight, blood flow rate, and the binding in blood and tissues. To clarify which factors have the greatest influence on the therapeutic index of capecitabine, one possible strategy is to predict the pharmacokinetics in humans from data obtained in animals. In fact, capecitabine is sequentially metabolized to 5-FU in mice and monkeys as well as in humans (5), and its antitumor activity has been observed in human cancer xenograft models (6– 8). However, in view of the sequential and organ-specific metabolism, which exhibits large inter-species differences (5), it will be difficult to predict the pharmacokinetics of capecitabine and its metabolites in humans from data in animals using the conventional animal scale-up method just based on the allometric relationship with body weight (9,10).

It should also be noted that, inter-patient variability has been observed in the activity of cyd deaminase and dThdPase in human tumor tissues (1). The tumor size and blood flow rate in tumor tissue also exhibit great inter-patient variability (11). Knowledge of the impact of such variable parameters on the therapeutic index will be important in developing tailor-made treatments with capecitabine for individual patients.

Another possible approach for predicting pharmacokinetics in humans is physiologically based pharmacokinetic (PBPK) modeling. The parameters for this modeling can be obtained from the literature or determined *in vitro*. The PBPK model has been applied successfully to the pharmacokinetics of chemotherapeutic agents, such as methotrexate, doxorubicin, and ara-C (12–14). However, most of the studies reported describe only the disposition of the parent drugs. Although some studies have dealt with the kinetics of a metabolite and a prodrug (15,16), no attempt has been made to

[1] Department of Preclinical Science, Nippon Roche Research Center, 200 Kajiwara, Kamakura, Kanagawa 247-8530, Japan.
[2] Department of Oncology, Nippon Roche Research Center, 200 Kajiwara, Kamakura, Kanagawa 247-8530, Japan.
[3] Graduate School of Pharmaceutical Sciences, University of Tokyo, Hongo, Bunkyo-ku, Tokyo 113-0033, Japan.
[4] To whom correspondence should be addressed at Graduate School of Pharmaceutical Science, University of Tokyo, Hongo, Bunkyo-ku, Tokyo 113-0033, Japan. (e-mail: sugiyama@mol.f.u-tokyo.ac.jp)

0724-8741/01/0800-1190$19.50/0 © 2001 Plenum Publishing Corporation

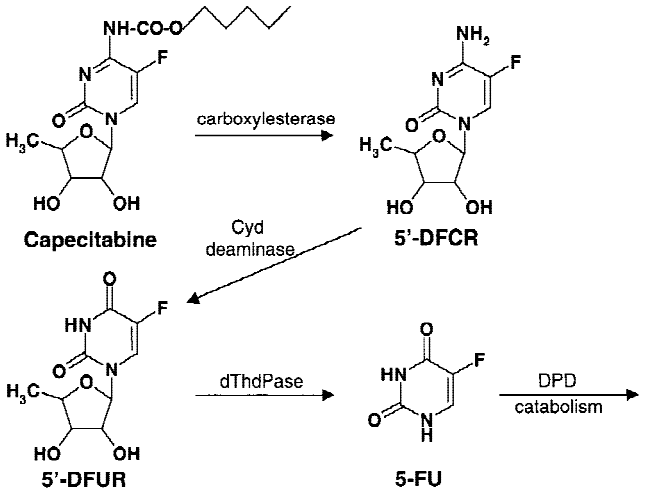

Fig. 1. Themetabolic pathway of capecitabine to 5-FU. Cyd deaminase; cytidine deaminase, dThdPase; thymidine phosphorylase, DPD; dihydropyrimidine dehydrogenase.

extend this method to triple prodrugs. In the present study, we have developed a PBPK model to describe the pharmacokinetics of capecitabine, 5′-DFCR, 5′-DFUR, and 5-FU in humans. To estimate the biochemical parameters required for this model, we measured the enzyme kinetic parameters, as well as the plasma and tissue binding of each compound in a series of *in vitro* studies. A sensitivity analysis was performed to identify the factors that influence the area under the curve (AUC) of 5-FU in tumor tissue and the GI as indices of the pharmacological effect and side effects of capecitabine, respectively. The pharmacokinetics of both doxifluridine (an oral prodrug of 5-FU) and 5-FU were also simulated to compare the characteristics of 5-FU pharmacokinetics among them.

MATERIALS AND METHODS

Materials

5-FU and [$^{15}N_2$]-5-FU were purchased from the Tokyo Kasei Co. (Tokyo, Japan) and C/D/N Isotopes (Quebec, Canada), respectively. 5′-DFUR was obtained from F. Hoffmann-La Roche (Basel, Switzerland). [^{13}C, $^{15}N_2$]-5′-DFCR,[$^{15}N_2$]-5′-DFUR, and [^{13}C, $^{15}N_2$]-capecitabine were supplied from Hoffmann-La Roche (NJ, USA). Capecitabine and 5′-DFCR were synthesized by Nippon Roche K.K. Research Center (Kamakura, Japan). Three human liver S9 (HHS-241, HHS-242, and HHS-245) and cytosol (HHC-241, HHC-242, and HHC-245), and human jejunal cytosol (HJC-0026, HJC-0033, and HJC-0036) prepared from intestinal mucosa, were purchased from the International Institute for the Advancement of Medicine (PA, USA). Human jejunal tissue (S-3891, S-3893, S-3894) were purchased from Kamiya Biochemical Company (WA, USA) and human jejunal S9 was prepared according using the method described by Miwa *et al.* (1). Part of the jejunal tissue were homogenized with a glass homogeniser in 4 volumes of 10 mM potassium phosphate buffer (pH 7.4) containing 1 mM 2-mercaptoethanol. The homogenate was centrifuged at 9,000 g for 20 min. The supernatant was dialyzed overnight against the same buffer and kept at –80°C until the enzyme activity analysis.

Kinetic Studies of Enzymatic Activities

Carboxylesterase, Cyd deaminase, and dThdPase activity were measured according to the method reported by Miwa *et al.* (1). Carboxylesterase activity was measured by determining the concentrations of the products formed from the substrate, capecitabine (0.3–10 mM). The assay mixture consisted of 160 mM potassium phosphate buffer (pH 7.4) containing 0.4 mM tetrahydrouridine (an inhibitor of cyd deaminase), 0.5 mM 2-mercaptoethanol, enzyme solution (2 mg protein/mL of human liver or jejunal S9), and capecitabine solution in a final volume of 50 μL. Inhibition of carboxylesterase activity by 2-mercaptoethanol was previously reported (17), but its effective concentration (~1% w/v) was more than 100 times higher. Cyd deaminase and dThdPase activity was measured by determining the concentrations of the products formed from 5′-DFCR (0.3–10 mM) and 5′-DFUR (0.1–3 mM), respectively. The assay mixture consisted of 160 mM potassium phosphate buffer (pH7.4) containing 0.5 mM 2-mercaptoethanol, enzyme solution (1 mg protein/mL of human liver or jejunal cytosol), and substrate in a final volume of 50 μL. The above three enzyme incubations were performed at 37°C for 60 min, and terminated by the addition of 300 μL of methanol. DPD activity was measured by determining the elimination of 5-FU (0.3–10 μM). The assay mixture consisted of 10 mM potassium phosphate buffer (pH 8.0) containing 0.5 mM EDTA, 0.5 mM 2-mercaptoethnol, 2 mM dithiothreitol, 2.5 mM $MgCl_2$, 250 μM NADPH, enzyme solution (1 mg protein/mL of human liver or jejunal cytosol), and 5-FU in a final volume of 50 μL. The enzyme solution was a mixture of the three cytosol preparations. Incubations were performed at 37°C for 0, 2, 5, and 15 min, and terminated by the addition of 300 μL of methanol. All the reaction mixtures were centrifuged at 1,000 g for 2 min and the supernatant obtained was dried under nitrogen gas, and the residue then dissolved in 200 μL water. The amount of 5′-DFCR, 5′-DFUR, and 5-FU was determined by selective liquid chromatography/ion spray ionization mass spectrometry (LC/MS/MS) as previously (5). The kinetic parameters (K_m, V_{max}) were determined from Eadie–Hofstee fitting of the enzymatic reactions data. The V_{max} values were shown as product amounts/min/g tissue by multiplying product amounts/min/mg protein by recoveries of mg protein from g tissue. The recoveries were 35.1, 113, 64.5, and 47.6 mg protein/g tissue for carboxylesterase activity and 11.7, 70.1, 55.6, and 38.3 mg protein/g tissue for cyd deaminase, dThdPase, and DPD activities in the GI, liver, colorectal cancer, and breast cancer tissues, respectively.

Blood-to-Plasma Concentration Ratio (R_B) and Plasma Protein

[^{14}C]-capecitabine, [^{14}C]-5′-DFCR, 5′-DFUR, or 5-FU was added to 2.5-mL aliquots of human blood to give a final concentration of 2 μg/mL. After incubation for 5 min at 37°C, a 200-μL aliquot was taken from each blood sample to measure the blood concentration. The remaining blood sample was centrifuged at 1,000 g for 10 min, and then 200 μL of plasma was used to measure the plasma concentration. An 800-μL aliquot of plasma was transferred to an ultrafiltration

tube (ULTRACENT-10, TOSOH, Tokyo, Japan) and the tubes centrifuged at 1,000 g (at 37°C), and then a portion of the filtrate was taken to measure the free concentration. The samples for the measurement of capecitabine, and 5′-DFCR were subjected to liquid scintillation counting. The samples for the measurement of 5′-DFUR and 5-FU were subjected to analysis by LC/MS/MS after deproteinazation with acetonitrile. The free fractions in blood (f_B) were calculated by dividing the free fractions in plasma by R_B.

Tissue Binding Study

To 2.5-mL aliquots of 33% mouse tissue homogenate, capecitabine, 5′-DFCR, 5′-DFUR, or 5-FU was added to give a final concentration of 2 μg/mL. After incubation for 10 min in iced water, the homogenate samples were transferred to ultrafiltration tubes (Ultracent-10, Tosoh, Tokyo, Japan). The tubes were centrifuged at 1,000 g (at 4°C), and then a portion of filtrate was taken from each tube to measure the free concentration. The samples were subjected to LC/MS/MS analysis after precipitation of protein with acetonitrile. The binding ratio in tissue was estimated by extrapolation of the tissue-binding ratio in 33% tissue homogenate to that in 100% tissue homogenate (18). The free fraction in tissue (f_T) was determined by subtracting the binding ratio from unity. The tissue-to blood concentration ratio (K_p) was estimated by dividing f_B by f_T. The tissue-to-unbound blood concentration ratio ($K_{p,u}$) was calculated by dividing the K_p value by f_B.

Model Development

A PBPK model was developed to describe the pharmacokinetics of capecitabine, 5′-DFCR, 5′-DFUR, and 5-FU in humans (Fig. 2). The key assumptions in this model were: (i) rapid equilibrium distribution of capecitabine and its metabolites between blood and tissues and (ii) sequential metabolism within a compartment according to a Michaelis–Menten process.

For capecitabine in the blood, GI, liver, tumor, and other tissue [non-eliminating tissue (NET) such as skin and muscle] compartments, the following Eq. (1) to (5), respectively, apply.

$$\frac{dC_{11}}{dt} = \left\{ (Q_2 + Q_3) \times \frac{C_{31}}{Kp_{31}} + Q_4 \times \frac{C_{41}}{Kp_{41}} + Q_5 \times \frac{C_{51}}{Kp_{51}} - Q_1 \times C_{11} - CL_{r,u} \times f_{B1} \times C_{11} \right\} / V_1 \quad (1)$$

$$\frac{dC_{21}}{dt} = \left\{ ka \times F \times X + Q_2 \times C_{11} - \left(Q_2 + \frac{\alpha_1 \times V_{max_{21}} \times f_{B1} \times V_2}{K_{m_{21}} + f_{B1} \times \frac{C_{21}}{Kp_{21}}} \right) \times \frac{C_{21}}{Kp_{21}} \right\} / V_2 \quad (2)$$

$$\frac{dC_{31}}{dt} = \left\{ Q_2' \times C_{11} + Q_3 \times C_{11} + Q_2 \times \frac{C_{21}}{Kp_{21}} - \left(Q_2 + Q_3 + Q_2' + \frac{\alpha_1 \times V_{max_{31}} \times f_{B1} \times V_3}{K_{m_{31}} + f_{B1} \times \frac{C_{31}}{Kp_{31}}} \right) \times \frac{C_{31}}{Kp_{31}} \right\} \quad (3)$$

$$\frac{dC_{41}}{dt} = \left\{ Q_4 \times C_{11} - \left(Q_4 + \frac{\alpha_1 \times V_{max_{41}} \times f_{B1} \times V_4}{K_{m_{41}} + f_{B1} \times \frac{C_{41}}{Kp_{41}}} \right) \times \frac{C_{41}}{Kp_{41}} \right\} / V_4 \quad (4)$$

$$\frac{dC_{51}}{dt} = \left\{ Q_5 \times C_{11} - Q_5 \times \frac{C_{51}}{Kp_5} \right\} / V_5 \quad (5)$$

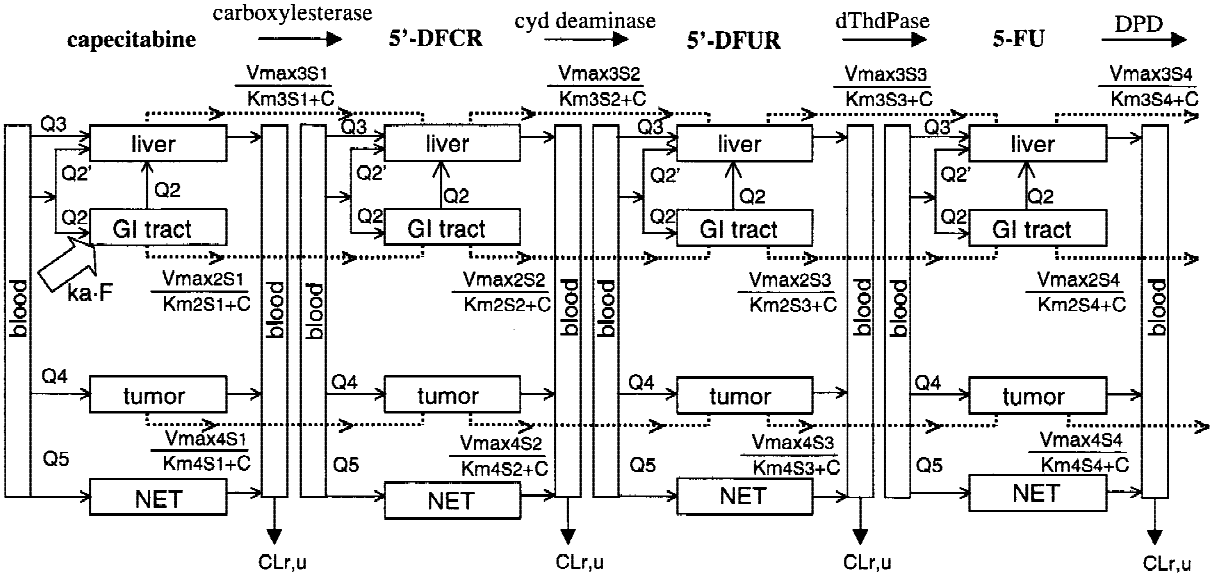

Fig. 2. PBPK model describing the pharmacokinetics of capecitabine and its metabolites after oral administration of capecitabine. The solid lines interconnecting compartments show the blood flow. The dotted lines show metabolic pathways. K_m and V_{max} are enzyme kinetic parameters: $K_{m(n)s1}$ and $V_{max(n)s1}$ for carboxylesterase, $K_{m(n)s2}$ and $V_{max(n)s2}$ for cyd deaminase, $K_{m(n)s3}$ and $V_{max(n)s3}$ for dThdPase, and $K_{m(n)s4}$ and $V_{max(n)s4}$ for for DPD, where n represents the number of the compartment (2, 3, 4, and 5 represent the GI, the liver, tumor tissue, and noneliminating tissues such as skin and muscle, respectively).

For metabolites in the blood, GI, liver, tumor, and NET compartments, respectively.

$$\frac{dC_{1n}}{dt} = \left\{ (Q_2 + Q_3) \times \frac{C_{3n}}{Kp_{3n}} + Q_4 \times \frac{C_{4n}}{Kp_{4n}} + Q_5 \times \frac{C_{5n}}{Kp_{5n}} - Q_1 \times C_{1n} - CL_{r,un} \times f_{Bn} \times C_{1n} \right\} / V_1 \quad (6)$$

$$\frac{dC_{2n}}{dt} = \left\{ Q_2 \times C_{1n} + \frac{\alpha_{(n-1)} \times V_{max_{2(n-1)}} \times f_{B(n-1)} \times V_2}{K_{m_{2(n-1)}} + f_{B(n-1)} \times \frac{C_{2(n-1)}}{Kp_{2(n-1)}}} \times \frac{C_{2(n-1)}}{Kp_{2(n-1)}} - \left(Q_2 + \frac{\alpha_n \times V_{max_{2n}} \times f_{Bn} \times V_2}{K_{m_{2n}} + f_{Bn} \times \frac{C_{2n}}{Kp_{2n}}} \right) \times \frac{C_{2n}}{Kp_{2n}} \right\} / V_2 \quad (7)$$

$$\frac{dC_{3n}}{dt} = \left\{ Q_2' \times C_{1n} + Q_3 \times C_{1n} + Q_2 \times \frac{C_{2n}}{Kp_{2n}} + \frac{\alpha_{(n-1)} \times V_{max_{3(n-1)}} \times f_{B(n-1)} \times V_3}{K_{m_{3(n-1)}} + f_{B1} \times \frac{C_{3(n-1)}}{Kp_{3(n-1)}}} \times \frac{C_{3(n-1)}}{Kp_{3(n-1)}} - \left(Q_2 + Q_2' + Q_3 + \frac{\alpha_n \times V_{max_{3n}} \times f_{Bn} \times V_3}{K_{m_{3n}} + f_{Bn} \times \frac{C_{3n}}{Kp_{3n}}} \right) \times \frac{C_{3n}}{Kp_{3n}} \right\} / V_3 \quad (8)$$

$$\frac{dC_{4n}}{dt} = \left\{ Q_4 \times C_{1n} + \frac{\alpha_{(n-1)} \times V_{max_{4(n-1)}} \times f_{B(n-1)} \times V_4}{K_{m_{4(n-1)}} + f_{B(n-1)} \times \frac{C_{4(n-1)}}{Kp_{4(n-1)}}} \times \frac{C_{4(n-1)}}{Kp_{4(n-1)}} - \left(Q_4 + \frac{\alpha_n \times V_{max_{4n}} \times f_{Bn} \times V_4}{K_{m_{4n}} + f_{Bn} \times \frac{C_{4n}}{Kp_4}} \right) \times \frac{C_{4n}}{Kp_{4n}} \right\} / V_4 \quad (9)$$

$$\frac{dC_{5n}}{dt} = \left(Q_5 \times C_{1n} - Q_5 \times \frac{C_{5n}}{Kp_{5n}} \right) / V_5 \quad (10)$$

Where C, $CL_{r,u,}$ ka, X, and F represented the concentration, renal clearance for unbound drug, absorption rate constant, amount of capecitabine in the GI luminal compartment where the drug is administered, and fraction of absorption, respectively. The n of subscript indicates each metabolite: the n = 2, 3, and 4 represent 5′-DFCR, 5′-DFUR, and 5-FU, respectively. V_n (n = 1 to 5) represents the organ volume. The α1 to α4 were the factors used for scaling from *in vitro* enzyme activities to *in vivo* for carboxylesterase, cyd deaminase, dThdPase, and DPD, respectively, these values being obtained by fitting as described below. The αi (i = 1 to 4) values were assumed to be the same among the tissues (liver, GI, and tumor).

The differential equation for the input of the drug to the body is shown in eq.11

$$\frac{dX}{dt} = -ka \times F \times X \quad (11)$$

where X at t = 0 (initial condition) is Dose.

Model Parameters

The physiologic parameters used in the model were obtained from the literature (19–22) and shown in Table I. For the blood flow rate in the GI, the mucosal blood flow rate was used as Q2 instead of the total intestinal blood flow rate as proposed by Klippert *et al.* (23). Consequently, the blood flow to the liver can be divided into three flows, hepatic artery blood flow (Q3), mucosal blood flow (Q2), and GI blood flow, apart from Q2 (Q2′). The $CL_{r,u}$ of capecitabine, 5′-DFCR, 5′-DFUR, and 5-FU in humans was calculated by dividing the amount excreted in the urine by the corresponding unbound AUC derived from the data reported by Judson *et al.* (24). The K_m was obtained in the present study. The V_{max} in tumor tissues were estimated from data obtained in the colorectal tumors of cancer patients reported by Miwa *et al.* (1) and Mori *et al.* (25) using as K_m values those obtained in the present study. The K_p values of capecitabine, 5′-DFCR, and 5′-DFUR in tumors were set at unity from the results of an uptake study using tumor cells, HCT116 and that of 5-FU in tumor was set at 2, following the report by Ojugo *et al.* (26) (Table II).

Model Fitting

The first fitting process was a simultaneous estimation by a nonlinear least squares fit of the model to the blood concentration data of capecitabine and its metabolites (24). The input data were weighted as the reciprocal of the square of the observed values using the nonlinear regression analysis

Table I. Physiologic Parameters

Organ	Blood flow rate (mL/min/kg)	Volume (mL/kg)
Blood	36.1[g]	85.6[a]
Including rapidly equilibrating tissues (kidneys, heart)		
Liver	16.5[f]	21.4[a]
GI	4.6[e]	23.6[c]
Tumor	0.0714[d]	0.286[b]
NET	15.0[c]	611[c]
Noneliminating tissues (muscle, skin)		

[a] From Benowitz *et al.* (19).
[b] From Zhu *et al.* (20).
[c] From Davis *et al.* (21).
[d] 0.25 mL/min/g tissue from Vaupel *et al.* (11).
[e] Mucosal blood flow rate in GI from Chiba *et al.* (22).
[f] The sum of hepatic artery blood flow (5.4 mL/min/kg) (19) and GI blood flow rate (15.7 mL/min/kg) (19) subtracted by mucosal blood flow rate in GI (22).
[g] The sum of blood flow rates in all organs included in the model shown in Fig. 2.

Table II. Kinetic Parameters for the Protein Binding, Tissue Distribution and Urinary Excretion of Capecitabine and Its Metabolites

Compound	f_B[a]	Kp[b]				$CL_{r,u}$[c,d] (mL/min/kg)
		GI[e]	Liver[e]	NET[f]	Tumor[g]	
Capecitabine	0.55 ± 0.03	0.90 ± 0.40	1.73 ± 0.20	0.56 ± 0.04	1	4.72 ± 0.93
5′-DFCR	0.95 ± 0.02	2.61 ± 0.09	1.46 ± 0.41	0.90 ± 0.05	1	3.99 ± 3.20
5′-DFUR	0.79 ± 0.03	3.11 ± 1.05	1.79 ± 0.57	0.46 ± 0.08	1	3.03 ± 1.42
5-FU	1.00 ± 0.07	1.71 ± 0.13	2.78 ± 0.80	0.56 ± 0.12	2[h]	2.38 ± 0.52

[a] Blood unbound fraction calculated as f_p/R_B.
[b] Tissue-to-blood concentration ratio.
[c] Urinary clearance defined to unbound blood concentration.
[d] Calculated from the data from Judson *et al.* (24).
[e] Determined from the binding study in each tissue homogenate.
[f] Obtained from the fitting procedure based on the data from Judson *et al.* (24).
[g] Determined from the uptake study.
[h] Obtained from Ojugo *et al.* (26).

program Napp (27). The estimated parameters were the ka of capecitabine, the K_p values of capecitabine and its metabolites in NET, and α1, α2, α3, and α4.

RESULTS

Enzymatic Activity Assessed *in Vitro*

The Eadie–Hofstee plots for the enzyme activity in two types of tumor tissues (colorectal cancer and breast cancer) resulted in straight lines (Fig. 3), the estimated K_m values being similar for both tumor tissues (Table III). The V_{max} values for carboxylesterase, dThdPase, and DPD were different in two tumor tissues (Table III). The magnitude of the V_{max} for each type of enzyme activity in liver tissue was greater than that in small intestinal tissue (Table III), the K_m values were similar for the liver and small intestinal tissues. Carboxylesterase, cyd deaminase, and dThdPase had K_m values in the mM range whereas DPD had a K_m in the μM range (Table III).

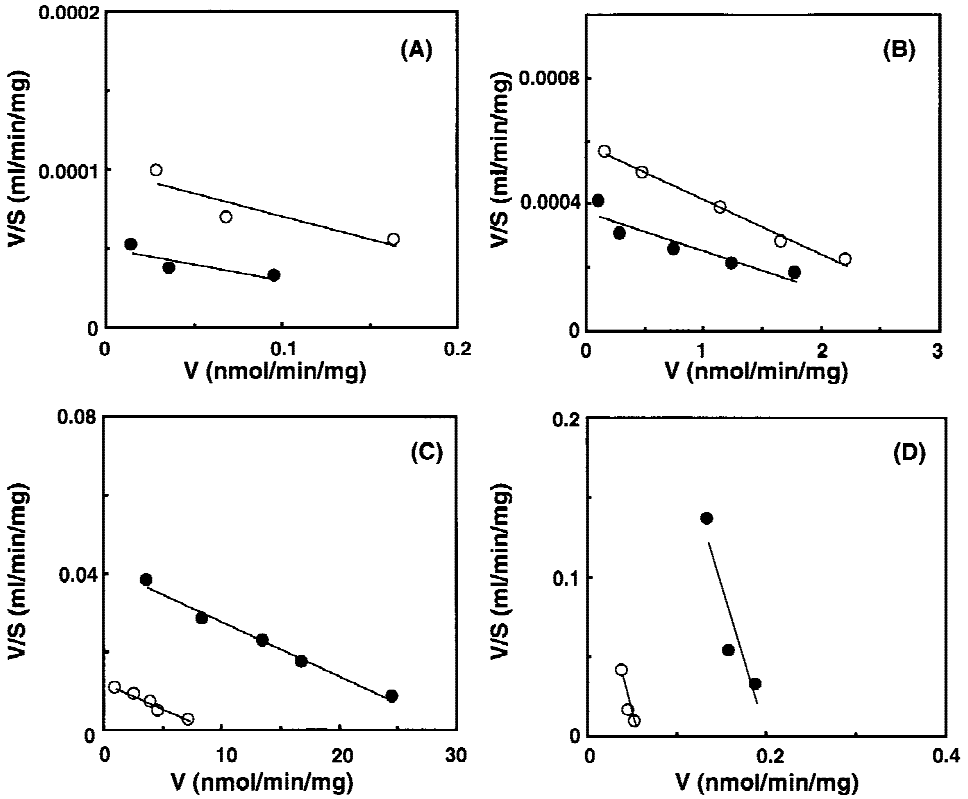

Fig. 3. Eadie–Hofstee plots for carboxylesterase (A), cyd deaminase (B), dThdPase (C), and DPD (D) in tumor tissues. The straight lines show the fitted line obtained by nonlinear least squares regression. In (A), (B), and (C), the data are shown as the mean of three independent subcellular fractions. In (D), the data were obtained by using the pooled sample from three independent tumors. ●, breast cancer tissue; ○, colorectal cancer tissue.

Table III. Kinetic Parameters of Metabolic Enzymes

	Carboxylesterase[a]		Cyd deaminase[a]		dThdPase[a]		DPD[b]	
Organ	K_m (nmol/mL)	V_{max} (nmol/min/g tissue)	K_m (nmol/mL)	V_{max} (nmol/min/g tissue)	K_m (nmol/mL)	V_{max} (nmol/min/g tissue)	K_m (nmol/mL)	V_{max} (nmol/min/g tissue)
GI tract	3160 ± 1650	5.34 ± 2.16	6470 ± 280	32.3 ± 16.1	522 ± 46	53.9 ± 4.4	1.67 ± 0.44	1.53 ± 0.15
Liver	6430 ± 1150	423 ± 137	5440 ± 580	401 ± 84	781 ± 52	642 ± 37	3.17 ± 0.77	22.5 ± 3.3
Tumor								
BC[c]	3740 ± 1380	8.84 ± 1.13	16900 ± 11800	166 ± 52	666 ± 96	1130 ± 710	0.454 ± 0.199	7.51 ± 0.65
CRC[d]	3170 ± 1340	20.6 ± 6.8	6810 ± 2530	192 ± 111	667 ± 156	474 ± 247	0.377 ± 0.129	3.06 ± 0.18

[a] Mean ± SD for the parameters obtained from three preparations.
[b] Mean ± calculated SD for the mixture of three S9 or cytosol preparations.
[c] Breast cancer.
[d] Colorectal cancer.

Renal Clearance of Capecitabine and Its Metabolites

The $CL_{r,u}$ for 5-FU were similar to the reported glomerular filtration rate (GFR) in humans (2 mL/min/kg) (19) whereas that of capecitabine, 5′-DFCR, and 5′-DFUR were slightly greater than the human GFR (Table II).

Construction of a PBPK Model and Its Validation

The fitted lines for the concentration/time curves of capecitabine, 5′-DFCR, 5′-DFUR, and 5-FU in blood were almost identical with the actual reported values (Fig. 4). The K_p values obtained by fitting for capecitabine, 5′-DFCR, 5′-DFUR, and 5-FU in NET were less than unity (0.56, 0.90, 0.46, and 0.56 respectively), suggesting that their tissue binding is low. The α values for carboxylesterase, cyd deaminase, dThdPase, and DPD activities were estimated as 80.6, 14.6, 1.30, and 3.14, respectively. Such α values higher than unity both for carboxylesterase and cyd deaminase suggests that the activity assessed *in vitro* does not represent that observed *in vivo*. Because this report dealt with only one substrate for each enzyme, further studies using other types of substrates are needed to establish the *in vitro* systems for these enzymes

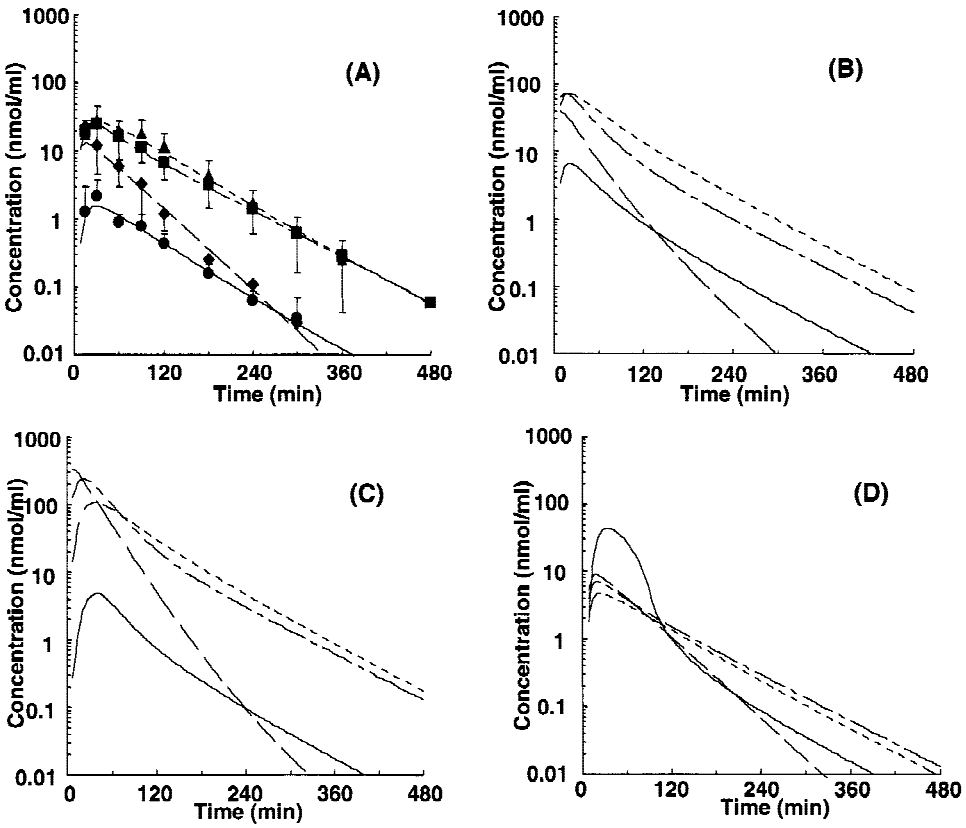

Fig. 4. Simulation for concentration/time profile of capecitabine, 5′-DFCR, 5′-DFUR, and 5-FU in blood (A), liver (B), GI (C), and colorectal cancer tissue (D). In (A), concentrations of capecitabine (♦), 5′-DFCR (■), 5′-DFUR (▲), and 5-FU (●) reported by Judson *et al.* (24) are also shown and converted from plasma concentrations by multiplying the plasma concentrations by R_B. — — —, capecitabine, - · - · , 5′-DFCR, – – –, 5′-DFUR, ——, 5-FU.

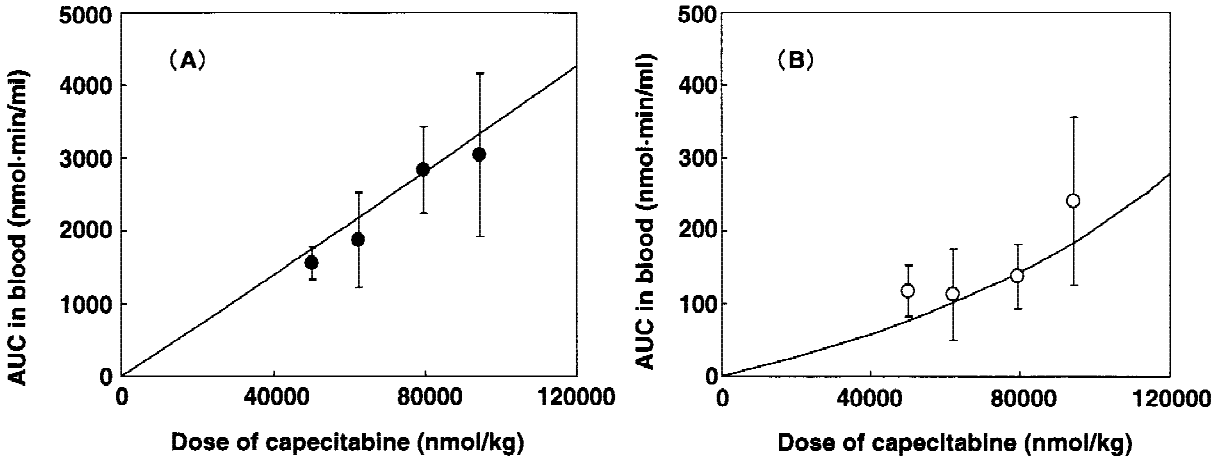

Fig. 5. Simulation for the dose dependency of blood 5′-DFUR (A) and 5-FU (B) AUC after oral administration of capecitabine. The solid lines show the simulated data. The AUC for 5′-DFUR (●) and 5-FU (○) was reported by Judson *et al.* (24), Budman *et al.* (28), Villalone-Calero *et al.* (29), Reigner *et al.* (30), and coverted to molar units multiplying by R_B (50,100 nmol/kg; 665.5 mg/m^2); Villalone-Calero *et al.,* 62,300 nmol/kg (828.5 mg/m^2); Budman *et al.,* 79,500 nmol/kg (1057 mg/m^2); Judson *et al.,* 94,400 nmol/kg (1255 mg/m^2); Reigner *et al.*).

to quantitatively estimate the *in vivo* activity. The concentration/time curves of capecitabine, 5′-DFCR, 5′-DFUR, and 5-FU in the liver, the GI, and tumor tissue were simulated based on the PBPK model (Fig. 4). The simulated 5-FU concentration profile in tumor was higher than that in blood and the GI (Fig. 4). The simulated increase in the AUC of 5′-DFUR and 5-FU in blood was relatively similar to the reported values (Fig. 5). A plot of 5′-DFUR AUC against the dose showed a straight line passing through the origin, while a plot for 5-FU AUC showed that it increased in a nonlinear manner (Fig. 5).

Effect of Enzyme Activity and Blood Flow Rate on the Tumor Exposure of 5-FU

Sensitivity analyses were performed to investigate the effect of the change in the enzyme activities on the pharmacokinetics of capecitabine and its active metabolite, 5-FU. In all the simulations shown here, the enzymatic activities (V_{max}) were varied from 0.1 to 10-fold the mean values. The carboxylesterase activities in the GI and liver affected the capecitabine AUC in blood, GI, liver, and tumor tissue (Fig. 6). The 5-FU AUC in blood and tumor tissue was only slightly influenced by a change of the four enzymes in the GI (Fig. 7). Only the 5-FU AUC in the GI itself was affected. The increase of the dThdPase activity in the liver caused a reduction in 5-FU AUC in the GI and tumor tissue (Fig. 7). The DPD activity in the liver markedly affected the 5-FU AUC in blood, GI, liver, and tumor tissue, whereas carboxylesterase and cyd deaminase in the liver had only a relatively minor effect (Fig. 7). In particular, a 100-fold change in the hepatic DPD activity caused a change in the 5-FU AUC of over 100-fold (Fig. 7).

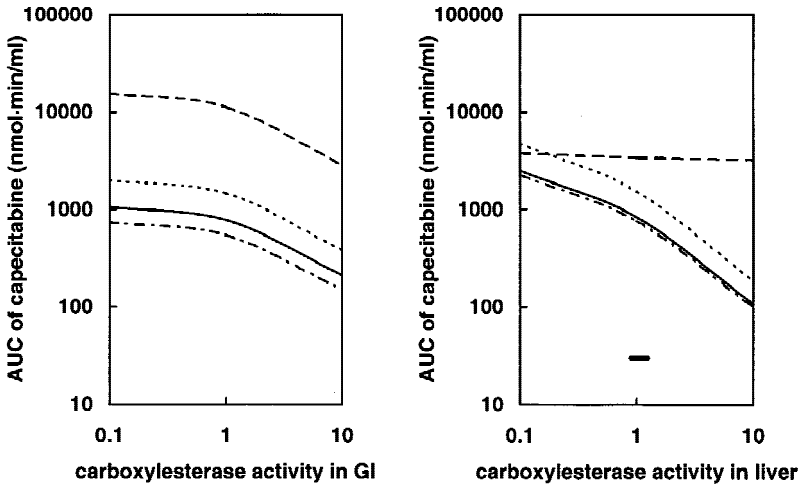

Fig. 6. Effect of carboxylesterase activity in GI and liver tissues on the capecitabine AUC in blood (——), the GI (— — —), the liver (– – –), and colorectal cancer tissue (– · –). The capecitabine AUCs were estimated by varying the carboxylesterase activity over a 0.1–10-fold range of the mean value. Bar: the 95% confidence interval of the mean V_{max} of carboxylesterase in human GI and liver from Miwa *et al.* (1).

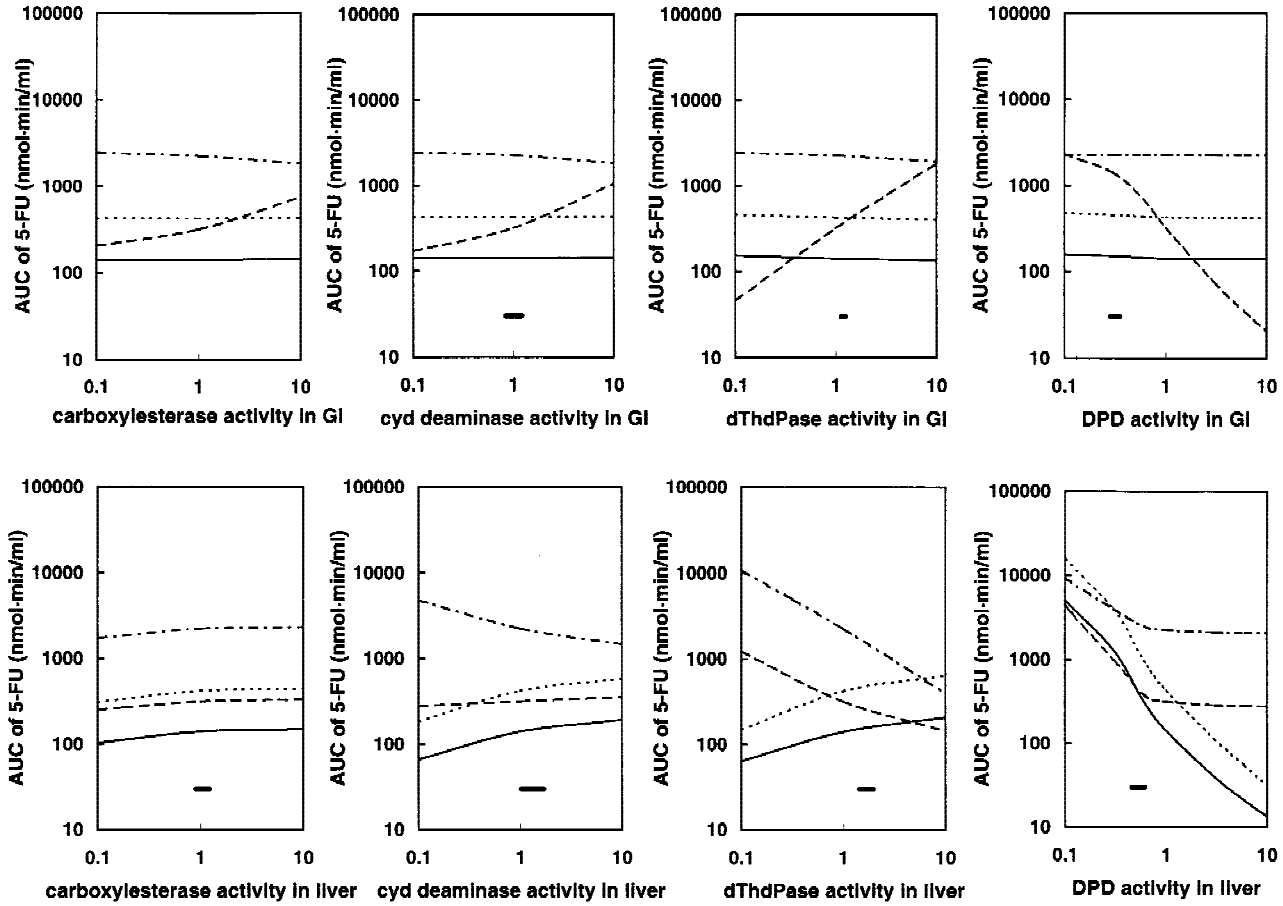

Fig. 7. Effect of activity of carboxylesterase, cyd deaminase, dThdPase, and DPD in GI and liver tissue on the 5-FU AUC. AUC in blood (——), the GI (— — —), the liver (– – –), and colorectal cancer tissue (– · –), the 5-FU AUCs were estimated by varying the activities of each enzyme over a 0.1–10-fold range of the mean value. Bar: the 95% confidence interval of the mean V_{max} of carboxylesterase, cyd deaminase, dThdPase, and DPD in human GI and liver from Miwa *et al.* (1).

The effects of the enzyme activities and the blood flow rate in the tumor on the 5-FU AUC was investigated (Fig. 8). Although the activity of both carboxylesterase and cyd deaminase were varied by over 10,000-fold range, the 5-FU AUC in tumor tissue was only slightly affected (Fig. 8). However, the 5-FU AUC in tumor tissue tended to increase with an increase in blood flow (Fig. 8). A change in the activity of dThdPase and DPD, on the other hand, markedly affected the 5-FU AUC in tumor tissue (Fig. 8). For all the blood flow rates examined, the reduction in 5-FU AUC was much more marked than the increase in DPD activity (Fig. 8), suggesting a nonlinear enzymatic reaction. A minimal change in the 5-FU AUC in the liver, GI or blood was observed on changing any of the enzyme activities in tumor tissue (data not shown). The 5-FU AUC was calculated (Fig. 9) using fixed enzyme parameters as the blood flow rate was altered within the reported range (Fig. 9). The 5-FU AUC in tumor tissue increased to markedly increasing the blood flow rate.

Comparison of Therapeutic Index Among Capecitabine and Other Fluoropyrimidines

The 5-FU AUC in blood, GI, and tumor tissues (Fig. 10) and the ratio of the 5-FU AUC in tumor tissue to that in GI (Fig. 11) were calculated after a single administration of capecitabine, doxifluridine (a simple prodrug of 5-FU), and 5-FU. Doxifluridine is given orally whereas 5-FU can be given either intravenously or orally in the chemotherapy of colorectal cancer. After oral administration of capecitabine, the 5-FU AUC increased in the following order: tumor > GI > blood over the clinical dose range from 829 to 1255 mg/m^2 (corresponding to 62,300 to 94,400 nmol/kg) (Fig. 10A). In tumor tissue, the 5-FU AUC increased by more than the increase in the dose of capecitabine (Fig. 10A). In blood and GI, such nonlinearity in the 5-FU AUC was relatively small (Fig. 10A). After a single oral administration of doxifluridine, a nonlinear increase in the 5-FU AUC in the GI was observed with an almost linear increase in that both in blood and tumor tissue over the clinical dose range (Fig. 10B). The 5-FU AUC in tumor tissue was similar to that in blood (Fig. 10B). The 5-FU AUC in tumor tissue was considerably lower than that in blood after a single oral or intravenous administration of 5-FU (Fig. 10C and 10D). In the case of oral administration of 5-FU, the 5-FU AUC in GI was considerably higher than that in blood and tumor tissues (Fig. 10C). This difference in the 5-FU AUC between GI and tumor tissue was relatively smaller after oral administration of doxifluridine (Fig. 10B). Thus, compared with 5-FU, doxifluridine appears to improve the accumulation of 5-FU in tumor tissue. Within the clinical dose range of doxifluridine and 5-FU, the AUC in tumor

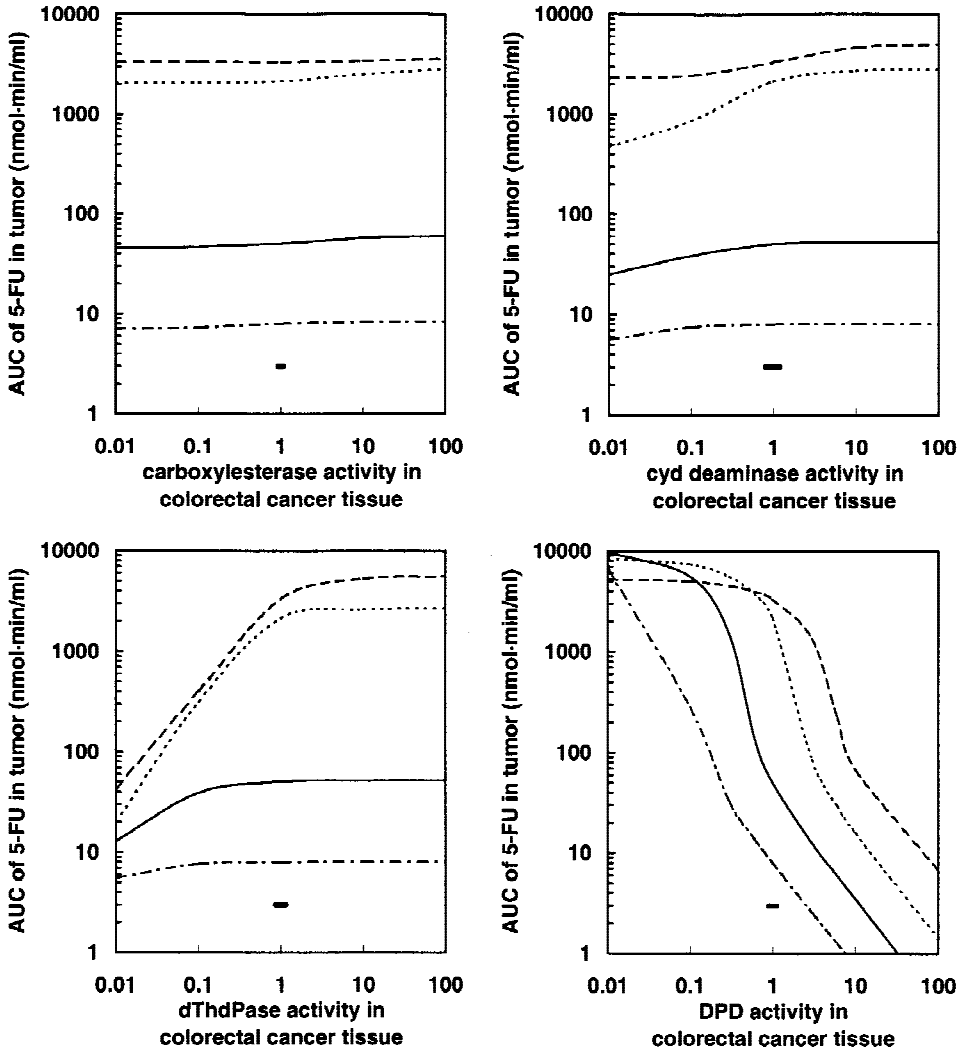

Fig. 8. Effect of the metabolic enzyme activities and blood flow rate in colorectal cancer tissue on the 5-FU AUC in tumor tissue. The activity of carboxylesterase, cyd deaminase, dThdPase, and DPD were varied over the range of 0.01-fold to 100-fold of the mean value for colorectal cancer tissue. The blood flow rates are fixed at 0.01 mL/min/g tissue (– · –), 0.05 mL/min/g tissue (——), 0.25 mL/min/g tissue (– – –), and 1.25 mL/min/g tissue (— — —). Bar: the 95% confidence interval of the mean V_{max} of each enzyme in colorectal cancer tissue from Miwa *et al.* (1) and Mori *et al.* (25).

tissue showed a slight degree of nonlinearity (Fig. 10B-D). After a single oral administration of capecitabine, doxifluridine, and 5-FU and continuous infusion of 5-FU, the ratio of the 5-FU AUC in tumor tissue to that in blood was 11.2–18.6, 0.85–0.87, 0.032–0.034, and 0.032–0.042, respectively. The ratio of the 5-FU AUC in tumor tissue to that in GI was also estimated to be 5.3-7.7, 0.039–0.030, 0.0002–0.0003, and 0.304–0.317, respectively, over the clinical dose ranges (Fig. 11, A and B).

DISCUSSION

Construction and Validation of the PBPK Model

Kinetic studies of the enzyme activities revealed that the V_{max} of carboxylesterase, cyd deaminase, and dThdPase in liver were higher than those in the small intestine (Table III). Miwa *et al.* (1) reported the highest activities of both cyd deaminase and dThdPase in the liver followed by the colorectum, stomach, and kidney, the activity in these extrahepatic tissues being approximately one third of that in the liver for cyd deaminase and approximately one third to one fifth of that in the liver for dThdPase (1). Thus, the present results are comparable with reported values. The V_{max} of DPD and carboxylesterase in liver were also higher than those in the small intestine, suggesting that the liver is the main organ involved in metabolism. In breast cancer tissue, the dThdPase activity per g tissue was approximately 2-fold higher than that in the liver, suggesting that this enzyme is highly expressed in this tumor tissue.

The blood and tissue protein binding of capecitabine and its metabolites were low (f_B values ranged from 0.55 to 1.00, K_p values ranged 0.90 to 3.11), indicating the minor contribution made by such binding to their pharmacokinetics. The simulated blood concentration profiles based on the parameters obtained by fitting were comparable with the reported data (24) (Fig. 4). The simulated blood AUCs of 5′-DFUR and 5-FU are consistent with the clinical observations (Fig. 5).

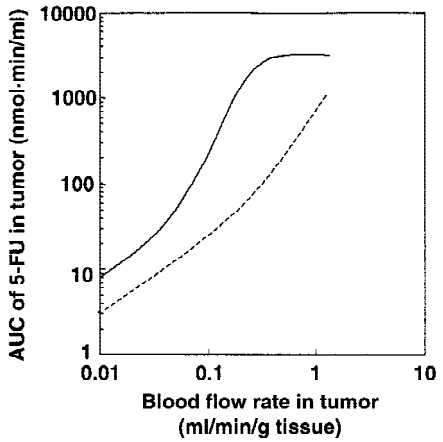

Fig. 9. Effect of blood flow rate in colorectal cancer and breast cancer tissues on the 5-FU AUC in tumor tissue. The AUC of 5-FU in tumor tissue was simulated based on the pharmacokinetic model shown in Fig. 2, where the kinetic parameters for enzyme activity were set at those obtained from colorectal cancer tissue (——) or breast cancer tissue (– – –).

These results suggest that the PBPK model is able to accurately describe the clinical data. Due to the limitations in the clinical data for the tissue concentration/time profile, further validation may be necessary to monitor the accuracy of each parameter. The K_m values of cyd deaminase for 5′-DFCR and dThdPase for 5′-DFUR were in the mM ranges (Table III) while, in the simulation, the estimated C_{max} value of 5′-DFCR and 5′-DFUR in the liver was in the μM range at a dose of 2,000 mg/body (5′-DFCR = 72.5 nmol/mL, 5′-DFUR = 70.3 nmol/mL). This suggests that these metabolic processes are linear over the clinical dose range of capecitabine, resulting in a linear increase in 5′-DFUR (Fig. 5). On the other hand, the K_m value of DPD for 5-FU in the liver was 3.17 nmol/mL (Table III) and the estimated C_{max} of 5-FU in the liver was 6.50 nmol/ml (Fig. 5). The maximum unbound 5-FU concentration in the liver ($f_B \cdot C_{max}/K_p = 2.86$ nmol/ml), was relatively similar to the Km value of DPD. This could be the reason for the nonlinearity in the 5-FU AUC (Fig. 5).

Factors Determining 5-FU AUC in Blood and Tissues

The metabolic enzymes in the GI only affected the 5-FU concentration in the GI (Figs. 6 and 7), whereas the hepatic DPD activity, followed by the hepatic cyd deaminase and dThdPase activities, had a marked effect on the 5-FU AUC (Fig. 7). Considering also that the metabolic activity in the liver is much higher than in the other organs, as discussed above, the key factor determining the 5-FU AUC in the systemic blood is the metabolic enzyme activity in the liver. It is notable that, compared with the other three enzymes, the systemic concentration of 5-FU was markedly affected by the

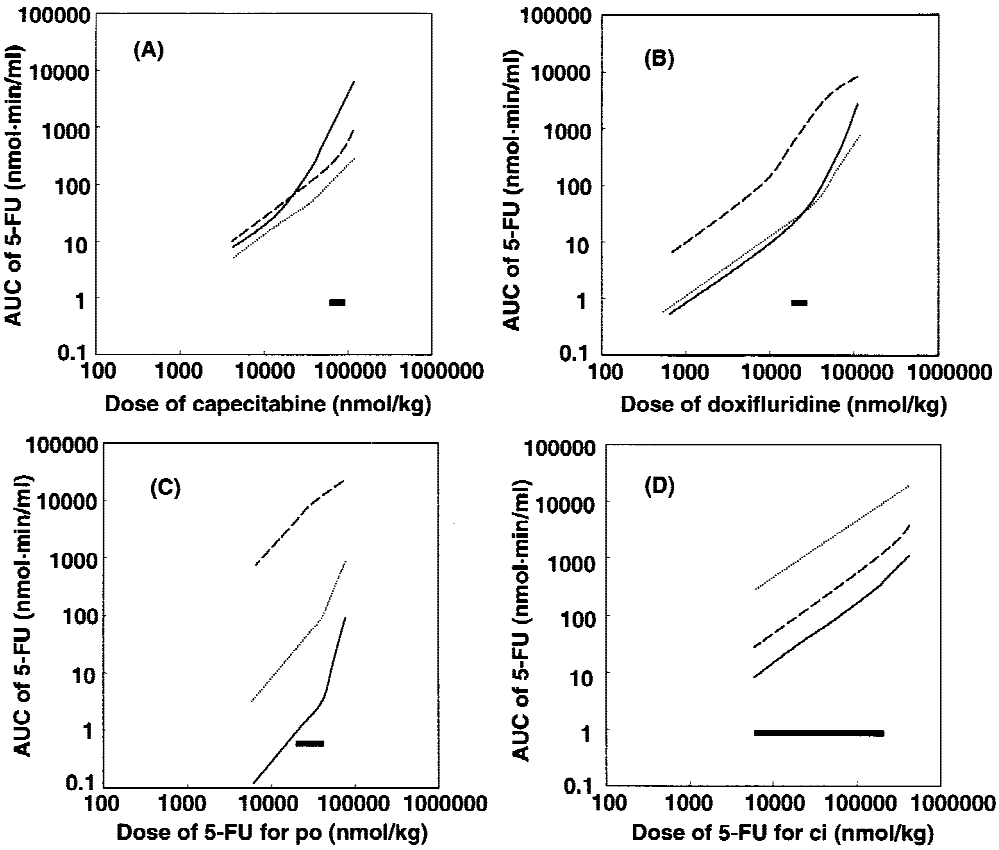

Fig. 10. Simulation for 5-FU AUC in blood (– – –), the GI (— — —), and tumor tissue (——) after administration of capecitabine, doxifluridine, and 5-FU in humans. The estimation was performed by assuming a patient (70 kg body weight) to have a tumor of 20 g. The bar shows the reported clinical dose range for each drug.

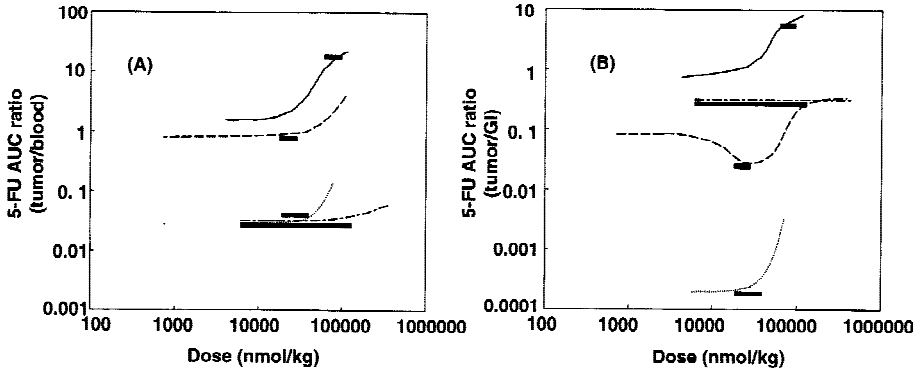

Fig. 11. The tumor-to-blood (A) and tumor-to-GI (B) ratio of 5-FU AUC after administration of capecitabine, doxifluridine, and 5-FU. The bar shows the reported clinical dose range for each drug. Capecitabine (p.o.), ——; doxifluridine (p.o.), — — —; 5-FU (continuous i.v.), – · –; 5-FU (p.o.), – – –.

DPD activity in liver (Fig. 7). The DPD in the GI also had a significant effect on the 5-FU AUC in the GI (Fig. 7). Because the affinity of DPD for 5-FU is high with a K_m in the μM range, saturation of this enzyme is likely to have an effect on 5-FU exposure in both the systemic and tissue compartments.

Compared with dThdPase and DPD, carboxylesterase and cyd deaminase have little effect on the 5-FU AUC in tumor tissue (Fig. 8), suggesting that the products of these enzymes, 5′-DFCR and 5′-DFUR, are mainly transported to tumor tissue by the systemic blood flow. This is compatible with another finding that the 5-FU AUC in tumor tissue increased with increasing blood flow rate, independently of any enzyme activity (Fig. 8), because of an increase in the supply of 5′-DFCR and 5′-DFUR. The reduction in 5-FU AUC in tumor tissue produced by the increase in dThdPase activity in the liver can also be explained by a reduction in the supply of 5′-DFUR by the systemic blood flow due to its extensive metabolism by the liver. On the other hand, dThdPase activity in tumor tissue markedly affects the 5-FU AUC (Fig. 8), suggesting that the activation of 5′-DFUR to 5-FU in tumor tissue makes a major contribution to the supply of 5-FU. The degree of the reduction in the 5-FU AUC in tumor tissue was greater than that of the increase in DPD activity in tumor tissue (Fig. 8). Considering both the C_{max} of 5-FU (40 μM) and its unbound fraction in tumor tissue (f_B/K_p = 0.45), its unbound concentration exceeded the K_m value of DPD (0.38–0.45μM). Such nonlinearity in the 5-FU AUC may be caused by saturation of DPD in tumor tissue. From these results, a greater pharmacologic effect of capecitabine should be observed in patients whose dThdPase activity in tumor tissue is high and DPD activity is low. This is compatible with the previous finding that capecitabine exhibits a potent pharmacological effect in human cancer xenograft models with a high ratio of dThdPase to DPD activity in tumor tissue (8). Sawada *et al.* (31) reported that combination of induction of dThdPase activity by X-ray irradiation and capecitabine was much more effective than either radiation or chemotherapy alone in human cancer xenograft models. The efficacy of capecitabine in tumors that have a low the dThdPase activity can be improved by taking capecitabine in addition to drugs and/or treatment that should enhance dThdPase activity.

Comparison of the Therapeutic Potential of Capecitabine with Other Fluoropyrimidines (5-FU and Doxifluridine)

The simulation based on the PBPK model revealed that oral administration of doxifluridine or capecitabine produces a drastic improvement in the accumulation of 5-FU in the tumor tissue compared with 5-FU itself (Fig. 11A). Doxifluridine is a prodrug of 5-FU, its conversion to 5-FU being mediated by dThdPase, which is highly expressed in tumor tissue. Such tumor-specific conversion may account for the greater amount of 5-FU reaching the tumor tissue. The tumor-to-blood ratio of 5-FU AUC (Fig. 11A) indicates that the targeting efficacy is much higher after oral capecitabine administration compared with doxifluridine. The GI toxicity is one of the dose-limiting factors of 5-FU. Therefore, the estimation of 5-FU exposure to the GI and its ratio to that in tumor tissue is important for evaluating the anticancer activity in patients. The ratio of the 5-FU AUC in tumor tissue to that in the GI after oral administration of doxifluridine was lower over the clinical dose range, compared with any other dose range (Fig. 11B) because of the nonlinear increase of the 5-FU AUC in the GI, possibly due to the first-pass effect (Fig. 10B). Such nonlinearity in the 5-FU AUC ratio was not observed with capecitabine (Fig. 11B). The ratio of the 5-FU AUC in tumor tissue to that in blood and the GI was estimated to be 18.6 and 7.7, respectively. Schüler *et al.* (4) have reported that the mean 5-FU concentration ratios of tumor tissue to blood and tumor tissue to GI were 21.4 and 3.21, respectively, in eleven colorectal cancer patients treated with capecitabine at a dose of 1255 mg/m^2. Thus, the therapeutic index of capecitabine is much higher than that of other fluoropyrimidines. This may be compatible with the very low gastrointestinal toxicity caused by capecitabine at the same dose as the clinical dose of doxifluridine (32). It should be noted that high tumor-specific accumulation of 5-FU after oral administration of capecitabine (Fig. 11) results from the marked nonlinear profile in the 5-FU AUC as was observed both in tumor tissue and the GI, the former being more pronounced (Fig. 10A), whereas the 5-FU AUC ratios are almost linear over the clinical dose ranges of the other fluoropyrimidines (Fig. 11). Such tumor-specific nonlinear 5-FU disposition is compatible with the finding that dThdPase and DPD in tumor tissue are important factors governing the 5-FU AUC in tu-

mor tissue. Thus, due to the tissue-specific sequential metabolic activation of capecitabine to 5-FU, the dose of capecitabine can be increased up to a level where saturation of 5-FU disposition can be observed in tumor tissue. In consequence, a higher therapeutic index should be observed after the administration of capecitabine compared with other fluoropyrimidines.

In conclusion, the pharmacokinetic behavior of capecitabine and its metabolites can be described by the PBPK model integrating the *in vitro* biochemical parameters measured in the present study. The simulation study revealed that the factors that significantly influence the 5-FU AUC in tumor tissue after oral administration of capecitabine are the activity of DPD and dThdPase, and the blood flow rate in tumor tissue. These parameters are highly relevant to the nonlinear accumulation of 5-FU in tumor tissue after oral administration of capecitabine compared with other fluoropyrimidine.

ACKNOWLEDGEMENTS

We thank Dr. Akihiro Hisaka (Drug Metabolism, Development Research Laboratories, Banyu Pharmaceutical Co Ltd) for supplying the nonlinear regression program Napp.

REFERENCES

1. M. Miwa, M. Ura, M. Nishida, N. Sawada, T. Ishikawa, K. Mori, N. Shimma, I. Umeda, and H. Ishitsuka. Design of a novel oral fluoropyrimidine carbamate, capecitabine, which generates 5-fluorouracil selectively in tumors by enzymes concentrated in human liver and tumor tissue. *Eur. J. Cancer* **34**:1274–1281 (1998).
2. R. B. Diaso and B. E. Harris. Clinical pharmacology of 5-fluorouracil. *Pharmacokinetics***16**:215–237 (1989).
3. S. P. Khor, H. Amyx, S. T. Davis, D. Nelson, D. P. Baccanari, and T. Spector. Dihydropyrimidine dehydrogenase inactivation and 5-fluorouracil pharmacokinetics: Allometric scaling of animal data, pharmacokinetics and toxicokinetics of 5-fluorouracil in humans. *Cancer Chemother. Pharmacol.* **39**:233–238 (1997).
4. J. Schüler, J. Cassidy, E. Dumont, B. Roos, S. Durston, L. Banken, M. Utoh, K. Mori, E. Weidekamm, and B. Reigner. Preferential activation of capecitabine in tumor following oral administration to colorectal cancer patients. *Cancer Chemother. Pharmacol.* **45**:291–297 (2000).
5. H. Onodera, I. Kuruma, H. Ishitsuka, and I. Horii. Pharmacokinetic study of capecitabine in monkeys and mice: Species differences in distribution of the enzyme responsible for its activation to 5-FU. *Xenobiol. Metabol. Dispos* **15**:439–451 (2000).
6. T. Ishikawa, Y. Fukase, T. Yamamoto, F. Sekiguchi, and H. Ishitsuka. Antitumor activities of a novel fluoropyrimidine, N^4-pentyloxycarbonyl-5′-deoxy-5-fluorocytidine (capecitabine). *Biol. Pharm. Bull.* **21**:713–717 (1998).
7. T. Ishikawa, M. Utoh, N. Sawada, M. Nishida, Y. Fukase, F. Sekiguchi, and H. Ishitsuka. Tumor selective delivery of 5-fluorouracil by capecitabine, a new oral fluoropyrimidine carbamate, in human cancer xenografts. *Biochem. Pharmacol.* **55**:1091–1097 (1998).
8. T. Ishikawa, F. Sekiguchi, Y. Fukase, N. Sawada, and H. Ishitsuka, Positive correlation between the efficacu of capecitabine and dosifluridine and the ratio of thymidine phsophorylase to dihydropymidine dehydorgenase activities in tumors in human cancer xenograft. *Cancer Res.* **58**:685–690 (1998).
9. R. L. Dedrick. Animal scale up. *J. Pharmacokinet. Biopharm.* **1**:435–461 (1973).
10. H. Boxenbaum. Interspecies variation in liver weight, hepatic blood flow, and antipyrine intrinsic clearance: extrapolation of data benzodiazepines and phenytoin. *J. Biopharmacokinet. Biopharm.* **8**:165–176 (1980).
11. P. Vaupel, F. Kallinowski, and P. Okunieff. Blood flow, oxygen and nutrient supply, and metabolic microenviroment of human tumors: a review. *Cancer Res.* **49**:6449–6465 (1989).
12. K. B. Bischoff, R. L. Dedrick, D. S. Zaharko, and J. A. Lonstreth. Methotrexate pharmacokientics. *J. Pharm. Sci.* **60**:1128–1133 (1981).
13. K. K. Chan, J. L. Cohen, J. F. Gross, K. J. Himmelstein, J. R. Bateman, Y. Tsu-Lee, and A. Marlis. Prediction of adriamycine disposition in cancer patients using a physiologic, pharmacokinetic model. *Cancer Treat. Rep.* **62**:1161–1171 (1978).
14. R. L. Dedrick, D. D. Forrester, J. N. Cannon, S. M. Dareer, and B. Mellett. Pharmacokinetics of 1-b-arabinofuranosyl cytosine (ARA-C) deamination in several species. *Biochem. Pharmacol.* **22**:2405–2417 (1973).
15. K. S. Pang. A review of metabolite kinetics. *J. Pharmacokinet. Biopharm.* **13**:633–662 (1985).
16. V. J. Stella and K. J. Himmelstein. Prodrug and site-specific drug delivery. *J. Med. Chem.* **23**:1275–1282 (1980).
17. K. Shirai, I. Ohsawa, Y. Saito, and S. Yoshida. Effects of phospholipids on hydrolysis of trioleoylglycerol by human serum carboxylesterase. *Biochim. Biophys. Acta* **962**:377–383 (1988)
18. J. H. Lin, Y. Sugiyama, S. Awazu, and M. Hanano. In vitro and in vivo evaluation of the tissue-to-blood partition coefficient for physiological pharmacokinetic models. *J. Pharmacokinet. Biopharm.* **10**:637–647 (1982).
19. N. Benowitz, R. P. Forsyth, K. L. Melmon, and M. Rowland. Lidocaine disposition kinetics in monkey and man. I. Prediction by a perfusion model. *Clin. Pharmacol. Ther.* **16**:87–98 (1974).
20. H. Zhu, R. J. Melder, L. T. Baxter, and R. K. Jain. Phsiologically based kinetic model of effect on cell biodistribution in mammals: implications for adoptive immunotherapy. *Cancer Res*. **56**:3771–3781 (1996).
21. B. Davis and T. Morris. Physiological parameters in laboratory animals and humans. *Pharm. Res.* **10**:1093–1095 (1993).
22. M. Chiba, M. Hensleigh, and J. H. Lin. Hepatic and intestinal metaboism of Indinavir, an HIV protease inhibitor, in rats and human microsomes, major role of CYP 3A. *Biochem. Pharmacol.* **53**:1187–1195 (1997).
23. P. Klippert, P. Borm, and J. Noordhoek. Predition of intestinal first-pass effect of phenacetine in the rat from enzyme kinetic data—Correlation with *in vivo* data using mucosal blood flow. *Biochem. Pharmacol.* **31**:2545–2548 (1982).
24. I. R. Judson, P. J. Beale, J. M. Trigo, W. Aherene, T. Cromptom, D. Jones, E. Bush, and B. Reigner. A human capecitabine excretion balance and pharmacokinetic study after administration of a single oral dose of $_{14}$C-labelled drug. *Invest. New Drugs* **17**:49–56 (1999).
25. K.Mori, M. Hasegawa, M. Nishida, H. Toma, M. Fukuda, T. Kubota, N. Nasue, H. Yamana, H. K. Chung, T. Ikeda, K. Tkasaki, M. Oka, M. Kameyama, M. Toi, H. Fujii, M. Kitayamura, M. Murai, H. Sasaki, S. Ozono, H. Mukuuchi, Y. Shimada, Y. Onhishi, S. Aoyagi, K. Mizutani, M. Ogawa, A. Nakao, H. Kinoshita, T. Tono, H. Imanoto, Y. Nakashima, and T. Manabe. Espression levels of thymidine phosphorylase and dihydropyrimidine dehydrogenase in various human tumor tissues. *Int. J. Oncol.* **17:**33–38 (2000).
26. A. S. E. Ojugo, P. M. J. McSheehy, M. Stubbs, G. Alder, C. L. Bashord, R. J. Maxwell, M. O. Leach, I. R. Judson, and J. R. Griffths. Influence of pH on the uptake of 5-fluorouracil into isolated tumor cell. *Br. J. Cancer* **77**:873–879 (1998).
27. A. Hisaka and Y. Sugiyama. Analysis of nonlinear and nonsteady state hepatic ectraction with the dispersion model using the finite difference method. *J. Phamacokinet. Biopharm.* **26**:495–519 (1998).
28. D. R. Budman, N. J. Meroopol, B. Reigner, P. J. Creaven, S. M. Lichtman, and E. Berghorn. Preliminary studies of a novel oral fluoropyrimidine carbamate: capecitabine. *J. Clin. Oncol*. **16**: 1795–1802 (1998).
29. M. A. Villalona–Calero, G. R. Weiss, H. A. Burris, M. Kraynak, G. Rodrigues, R. L. Dregler, S. G. Eckhardt, B. Reigner, J. Moczygembra, H. U. Burger, T. Griffin, D. D. Von Hoff, and E. K. Rowinsky. Phase I and pharmacokinetic study of the oral fluoropyrimidine capecitabine in combination with paclitaxel in pa-

tients with advanced solid malignancies. *J. Clin. Oncol.* **17**:1915–1925 (1999).
30. B. Reigner, J. Verweij, L. Dirix, J. Cassidy, C. Twelves, D. Allman, E. Weidekamm, B. Roos, L. Banken, M. Utoh, and B. Osterwalder. Effect of food on the pharmacokinetics of capecitabine and its metabolites following oral administration in cancer patients. *Clin. Cancer Res.* **4**:941–948 (1998).
31. N. Sawada, T. Ishikawa, F. Sekiguchi, Y. Tanaka, and H. Ishitsuka. X-ray irradiation induces thymidine phosphorylase and enhances the efficacy of capecitabine (Xeloda) in human cancer xenografts. *Clin. Cancer Res.* **5**:2948–2953 (1999).
32. M. Mackean, A. Planting, C. Twelves, J. Schellens, D. Allman, B. Osterwalder, B. Reigner, T. Griffin, S. Kaya, and J. Verweij. Phase I and pharmacologic study of intermittent twice-daily oral therapy with capoecitabine in patients with advanced and/or metastatic cancer. *J. Clin. Oncol.* **16**:2977–2985